

Gaseous (DMS, MSA, SO₂, H₂SO₄ and DMSO) and particulate (sulfate and methanesulfonate) sulfur species over the northeastern coast of Crete

H. Bardouki¹, H. Berresheim², M. Vrekoussis¹, J. Sciare^{3,4}, G. Kouvarakis¹, K. Oikonomou¹, J. Schneider³, and N. Mihalopoulos¹

¹Environmental Chemical Processes Laboratory (ECPL), Department of Chemistry, University of Crete, P.O Box 1470, 71409 Heraklion Greece

²Deutscher Wetterdienst (DWD), Meteorological Observatory, Hohenpeissenberg, Germany

³Max-Planck Institute for Chemistry, Biogeochemistry Division, Mainz, Germany

⁴now at LSCE, Orme des Merisiers, Bat 709, CE Saclay, 91191 Gif-sur-Yvette Cedex, France

Received: 21 April 2003 – Accepted: 4 July 2003 – Published: 25 July 2003

Correspondence to: N. Mihalopoulos (Mihalo@chemistry.uoc.gr)

Title Page

Abstract

Introduction

Conclusions

References

Tables

Figures

◀

▶

◀

▶

Back

Close

Full Screen / Esc

Print Version

Interactive Discussion

© EGU 2003

**Gaseous and
particulate sulfur
species**

H. Bardouki et al.

A detailed study of the levels, the temporal and diurnal variability of the main compounds involved in the biogenic sulfur cycle was carried out in Crete (Eastern Mediterranean) during the Mediterranean Intensive Oxidant Study (MINOS) field experiment in July–August 2001. Intensive measurements of gaseous dimethylsulfide (DMS), dimethylsulfoxide (DMSO), sulfur dioxide (SO_2), sulfuric (H_2SO_4) and methanesulfonic acids (MSA) and particulate sulfate (SO_4^{2-}) and methanesulfonate (MS^-) have been performed during the campaign.

Dimethylsulfide (DMS) levels ranged from 2.9 to $136 \text{ pmol}\cdot\text{mol}^{-1}$ (mean value of $21.7 \text{ pmol}\cdot\text{mol}^{-1}$) and showed a clear diurnal variation with daytime maximum. During nighttime DMS levels fall close or below the detection limit of $2 \text{ pmol}\cdot\text{mol}^{-1}$. Concurrent measurements of OH and NO_3 radicals during the campaign indicate that NO_3 levels can explain most of the observed diurnal variation of DMS. Dimethylsulfoxide (DMSO) ranged between 0.02 and $10.1 \text{ pmol}\cdot\text{mol}^{-1}$ (mean value of $1.7 \text{ pmol}\cdot\text{mol}^{-1}$) and presents a diurnal variation similar to that of DMS. SO_2 levels ranged from 220 to $2970 \text{ pmol}\cdot\text{mol}^{-1}$ (mean value of $1030 \text{ pmol}\cdot\text{mol}^{-1}$), while nss-SO_4^{2-} and MS^- ranged from 330 to $7100 \text{ pmol}\cdot\text{mol}^{-1}$, (mean value of $1440 \text{ pmol}\cdot\text{mol}^{-1}$) and 1.1 to $37.5 \text{ pmol}\cdot\text{mol}^{-1}$ (mean value of $11.5 \text{ pmol}\cdot\text{mol}^{-1}$) respectively.

Of particular interest are the measurements of gaseous MSA and H_2SO_4 . MSA ranged from below the detection limit (3×10^4) to 3.7×10^7 molecules cm^{-3} , whereas H_2SO_4 ranged between 1×10^5 and 9.0×10^7 molecules cm^{-3} . The measured H_2SO_4 maxima are among the highest reported in literature and can be attributed to high insolation, absence of precipitation and increased SO_2 levels in the area. From the concurrent SO_2 , OH, and H_2SO_4 measurements a sticking coefficient of 0.52 ± 0.28 was calculated for H_2SO_4 . From the concurrent MSA, OH, and DMS measurements the yield of gaseous MSA from the OH-initiated oxidation of DMS was calculated to range between 0.1–0.4%. This low MSA yield implies that gaseous MSA levels can not

[Title Page](#)[Abstract](#)[Introduction](#)[Conclusions](#)[References](#)[Tables](#)[Figures](#)[◀](#)[▶](#)[◀](#)[▶](#)[Back](#)[Close](#)[Full Screen / Esc](#)[Print Version](#)[Interactive Discussion](#)

© EGU 2003

account for the observed MS^- levels. Heterogeneous reactions of DMSO on aerosols should be considered to explain the observed levels of MS^- .

1. Introduction

Oceanic dimethylsulfide (DMS) emission is proposed to play a key role in climate regulation, through its oxidation products, especially in the remote marine atmosphere (Charlson et al., 1987). Once emitted into the atmosphere DMS can be oxidized by OH, NO_3 and possibly other radical species as Cl atoms and BrO radicals forming a variety of products such as sulfur dioxide (SO_2), methanesulfonic acid (MSA) and dimethylsulfoxide (DMSO) (e.g. Watts et al., 1990; Urbanski et al., 1998; Davis et al., 1998; Arsene et al., 1999 and references therein).

The proposed climatic impact of DMS is decisively determined from H_2SO_4 production contributing to the formation of new hygroscopic sulfate particles. On the other hand, the contribution of MSA, another main oxidation end-product of DMS, to new particle formation is expected to be negligible, at least in the polluted marine atmosphere (Kreidenweis and Seinfeld, 1988). Particles can play an important climatic role by scattering solar radiation and acting as cloud condensation nuclei (CCN), thus influencing the earth's albedo and climate (IPCC, 2001).

The complete mechanism of DMS oxidation is still under investigation although considerable effort has been made during the last decades to clarify its oxidation scheme via field measurements, kinetic experiments and model results (e.g., Berresheim et al., 1995 and references therein). From numerous field and laboratory experiments it is clear that the atmospheric distribution of DMS oxidation products critically depends on various factors like meteorology (temperature, humidity) and the oxidation power of the atmosphere (e.g. NO_x , HO_x).

Concurrent field data both on the oxidants involved in the DMS oxidation and including at least the major oxidation products of DMS in gaseous and particulate phase are clearly needed to validate the laboratory results. Such data is particularly difficult

Title Page

Abstract

Introduction

Conclusions

References

Tables

Figures

◀

▶

◀

▶

Back

Close

Full Screen / Esc

Print Version

Interactive Discussion

**Gaseous and
particulate sulfur
species**H. Bardouki et al.

[Title Page](#)[Abstract](#)[Introduction](#)[Conclusions](#)[References](#)[Tables](#)[Figures](#)[◀](#)[▶](#)[◀](#)[▶](#)[Back](#)[Close](#)[Full Screen / Esc](#)[Print Version](#)[Interactive Discussion](#)

© EGU 2003

to obtain since the levels of free radicals and DMS oxidation products are often very low (in sub-pmol·mol⁻¹ level) and state-of-the-art analytical techniques are needed. To our knowledge only few studies have fulfilled all the above requirements. Especially in the marine boundary layer only one study has been performed so far (the SCATE experiment in coastal Antarctica; Berresheim and Eisele, 1998). The MINOS campaign conducted in Crete in July–August 2001, provides the first comprehensive dataset to understand the factors controlling the distribution and the fate of DMS oxidation products under moderately polluted marine conditions. Intensive measurements of gaseous DMS, DMSO, SO₂, H₂SO₄ and MSA and particulate sulfate (SO₄²⁻) and methanesulfonate (MS⁻) have been performed during the campaign in conjunction with parallel measurements of OH (Berresheim et al., 2003) and NO₃ radicals (Vrekoussis et al., 2003).

2. Experimental

2.1. Location

All measurements reported here have been performed at Finokalia (35°24' N, 25°60' E), a remote location on the northern coast of Crete, Greece. The station is located at the top of an elevation (150 m) facing the sea within the sector of 270° to 90°. No significant anthropogenic sources exist at a distance shorter than 20 km within the above-mentioned sector. Details on the area and the meteorological conditions encountered year-round at Finokalia are given by Mihalopoulos et al. (1997) and Kouvarakis et al. (2000).

2.2. Sampling and analysis

DMS: Air sampling and subsequent analysis of DMS were carried out as described in previous studies (Nguyen et al., 1990; Sciare et al., 2001; Kouvarakis and Mihalopoulos

**Gaseous and
particulate sulfur
species**H. Bardouki et al.

[Title Page](#)[Abstract](#)[Introduction](#)[Conclusions](#)[References](#)[Tables](#)[Figures](#)[◀](#)[▶](#)[◀](#)[▶](#)[Back](#)[Close](#)[Full Screen / Esc](#)[Print Version](#)[Interactive Discussion](#)

© EGU 2003

los, 2002). Briefly, air was collected into 6-liter stainless steel canisters and pressurized up to 5 bars using a pump. As described by Kouvarakis and Mihalopoulos (2002), the use of such canisters minimizes possible DMS destruction by oxidants. Immediately after sampling DMS analysis was isothermally performed (95°C) by gas chromatography (HP 5890A GC equipped with a Chromosil 310 column and a flame photometric detector; FPD). The detection limit was typically 0.2 ng (DMS), which under our sampling conditions corresponds to 2 pmol·mol⁻¹ of DMS. The accuracy of the analysis was 10%. In total, 490 atmospheric DMS measurements were performed during the campaign (28 July to 22 August 2001) with an average sampling interval of 1 h.

DMSO and SO₂: The technique used for the sampling of atmospheric DMSO and SO₂ is based on the nebulization/reflux principle (Cofer et al., 1985; Sciare and Mihalopoulos, 2000). Two samplers were operated in parallel during the campaign (one for DMSO and the other for SO₂ and other water soluble gases) with an average flow rate of 16 L min⁻¹. After sampling the aliquots for DMSO and SO₂ analysis were kept refrigerated at 4°C in the dark and analyzed within a month period. Conservation tests have shown that both DMSO and SO₂ were stable under these storage conditions.

DMSO was reduced by sodium borohydride (NaBH₄) to DMS and subsequently analysed by gas chromatography. Recovery and reproducibility of the analysis were of the order of 90% and better than 10%, respectively. Details on the DMSO collection and analysis have been described by Sciare and Mihalopoulos (2000). In total, 201 atmospheric DMSO measurements have been performed during the campaign with an average sampling step of 3 hrs. The detection limit for a mean sampling volume of 3 m³ was found to be 0.03 pmol·mol⁻¹ and the precision was estimated to be 20%. Gaseous SO₂ (n=226) was trapped in aqueous droplets produced inside the sample mist chamber and analyzed as sulfate by Ion Chromatography (see details below). The Cofer mist technique has been successfully compared in the field against the alternative Na₂CO₃-impregnated filter technique (Sciare et al., 2003). The detection limit for a mean sampling volume of 3 m³ was found to be 20 pmol·mol⁻¹ and the precision was estimated to be 15%.

**Gaseous and
particulate sulfur
species**

H. Bardouki et al.

[Title Page](#)[Abstract](#)[Introduction](#)[Conclusions](#)[References](#)[Tables](#)[Figures](#)[◀](#)[▶](#)[◀](#)[▶](#)[Back](#)[Close](#)[Full Screen / Esc](#)[Print Version](#)[Interactive Discussion](#)

© EGU 2003

Aerosol (sulfate and methanesulfonate) sampling and analysis: Bulk aerosol samples were collected on $0.5\ \mu\text{m}$ PTFE filters. In total, 226 aerosol samples were collected during the sampling period in parallel with DMSO and SO_2 and subsequently analysed for the main anions and cations by Ion Chromatography.

For the analysis of anions (chloride: Cl^- ; bromide: Br^- ; nitrate: NO_3^- ; sulfate: SO_4^{2-} ; oxalate: $\text{C}_2\text{O}_4^{2-}$) a Dionex AS4A-SC column with ASRS-I suppressor in auto-suppression mode of operation was used and isocratic elution at $2.0\ \text{ml min}^{-1}$ of $\text{Na}_2\text{CO}_3/\text{NaHCO}_3$ eluent. MS^- was analyzed using a Dionex DX-500 Ion Chromatography with an AS11 analytical column and NaOH ($0.1\text{--}3.5\ \text{mM}$) as eluent in gradient mode. For the cations (sodium: Na^+ ; ammonium: NH_4^+ ; potassium: K^+ ; magnesium: Mg^{2+} and calcium: Ca^{2+}) a CS12-SC column was used with CSRS-I suppressor. Separation was achieved under isocratic conditions with $20\ \text{mM}$ MSA eluent and flow rate of $1.0\ \text{ml min}^{-1}$: The reproducibility of the measurements was better than 2% and the detection limit ranged from around 5 ppb for the main anions and cations to below 0.2 ppb for MS^- . More details on the analytical technique can be found in Baboukas et al. (2000) and Kouvarakis and Mihalopoulos (2002).

Atmospheric H_2SO_4 , MSA, and OH measurements: H_2SO_4 , MSA, and OH concentrations in the gas phase were measured by Deutscher Wetterdienst (DWD) using chemical ionization mass spectrometry (CIMS) based on methods previously developed by Eisele and coworkers (Tanner et al., 1997; Eisele and Tanner, 1993). The DWD CIMS system has been described in detail by Berresheim et al. (2000, 2002). At 5 min signal integration, the overall 2-sigma precisions and detection limits for both the H_2SO_4 and MSA measurements were 21% and 3×10^4 molecules cm^{-3} . For OH radicals the corresponding values were 22% and 2.4×10^5 molecules cm^{-3} (Berresheim et al., 2003).

Ancillary measurements: An optical particle counter (PCS 2010, Palas Inc.) was used to measure the size distribution of particles between 270 nm and $9\ \mu\text{m}$. The size distribution below 200 nm was measured with a TSI 3040 diffusion battery. The optical particle counter was installed in a measurement container which was deployed

approximately 30 m below the meteorological station. The total aerosol surface density was calculated from the data of both instruments. The gap between 200 and 270 nm could be closed by comparison with an aircraft based PCASP instrument (Schneider et al., 2003), which yielded a contribution of about 30% to the total surface from particles between 200 and 270 nm. The particles with diameters smaller than 200 nm contributed about 60% to the total aerosol surface density. Meteorological parameters like temperature, humidity, wind speed and direction were measured continuously by an automated meteorological station.

3. Results and Discussion

Table 1 summarizes the range, mean and standard deviation of concentrations of DMS and the other gaseous and particulate S species during the campaign. In the present section the variations and the factors controlling the levels of the gaseous and particulate S species measured during the campaign will be discussed. Preceding the presentation of the levels of the S compounds and the discussion of the factors controlling their levels, a summary of the aerosol surface and RH data is given in Fig. 1. Aerosol surface concentrations during the MINOS campaign ranged from 49 to 605 $\mu\text{m}^2 \text{cm}^{-3}$ (272 ± 120) and followed the variation of RH quite well ($r^2=0.21$, $p<0.001$).

3.1. DMS

DMS levels (Fig. 2a) range from values near the detection limit ($2.0 \text{ pmol}\cdot\text{mol}^{-1}$) to 136 $\text{pmol}\cdot\text{mol}^{-1}$ (on 31 July) with a mean value of $21.7 \text{ pmol}\cdot\text{mol}^{-1}$. They are in good agreement with the data reported for a coastal site in Israel measured during August 1995 ($22 \text{ pmol}\cdot\text{mol}^{-1}$; Ganor et al., 2000). The DMS values observed during MINOS fall in the lower range of summer values reported for the Finokalia area for the period 1997–1999 ($57.5 \pm 33.8 \text{ pmol}\cdot\text{mol}^{-1}$; Kouvarakis and Mihalopoulos, 2002). The relatively low DMS values observed during MINOS can be attributed to two possible fac-

[Title Page](#)[Abstract](#)[Introduction](#)[Conclusions](#)[References](#)[Tables](#)[Figures](#)[◀](#)[▶](#)[◀](#)[▶](#)[Back](#)[Close](#)[Full Screen / Esc](#)[Print Version](#)[Interactive Discussion](#)

**Gaseous and
particulate sulfur
species**

H. Bardouki et al.

[Title Page](#)[Abstract](#)[Introduction](#)[Conclusions](#)[References](#)[Tables](#)[Figures](#)[⏪](#)[⏩](#)[◀](#)[▶](#)[Back](#)[Close](#)[Full Screen / Esc](#)[Print Version](#)[Interactive Discussion](#)

© EGU 2003

tors: 1) Lower wind speed during the campaign (7.1 m s^{-1}) than the summertime mean value derived from long term measurements (9 m s^{-1} ; Kouvarakis et al., 2000). Such difference in wind speed can affect the transfer (or piston) velocity (K_w) of DMS and consequently DMS sea-to-air fluxes by almost 50% (Liss and Merlivat, 1986). 2) Land breeze occurrence during nighttime (see also Berresheim et al, 2003, this issue). This rather unusual situation for the area, resulted in a dilution of oceanic DMS flux during night by a factor of 30% compared to the daytime flux (see the companion modelling paper by Kanakidou et al., 2003, this issue). Figure 2b depicts the diurnal variation of normalized DMS (Normalized DMS= $\text{DMS}_{(\text{time}_y, \text{day}_x)}/\text{mean DMS}_{(\text{day}_x)}$) during the experiment. Measurements of OH and NO_3 radicals, averaged during the entire campaign, are also reported in Fig. 2b. DMS presents a well-defined diurnal variation with high values during daytime and a clear minimum (in most cases near to the detection limit) during night with a day to night amplitude of 5.4. Based on the observed levels of OH and NO_3 radicals, the nighttime DMS minimum is attributed to dilution due to land-to-sea breeze occurrence and the reaction of DMS with NO_3 radicals. The minimum observed around 15:00 (LT), can be explained by/attributed to the DMS+OH reaction. Finally the increase observed around 18:00 can be explained by the absence of significant levels of both radicals. A detailed modeling study of the diurnal variation of DMS is presented in Kanakidou et al. (2003). The DMS diurnal variation is in agreement with previous observations during summertime at Finokalia (Kouvarakis and Mihalopoulos, 2002) and observations in the marine atmosphere under continental influence (e.g. Andreae et al. 1985). However, it is different from those observed in the remote marine atmosphere (Andreae et al., 1985; Ayers et al., 1995; Sciare et al., 2001) where a clear DMS minimum is observed around noon time.

3.2. DMSO

DMSO is one of the major intermediate DMS oxidation products. In the gas phase it is produced through the OH-addition channel, with a yield of approximately 30% of the

**Gaseous and
particulate sulfur
species**

H. Bardouki et al.

[Title Page](#)[Abstract](#)[Introduction](#)[Conclusions](#)[References](#)[Tables](#)[Figures](#)[◀](#)[▶](#)[◀](#)[▶](#)[Back](#)[Close](#)[Full Screen / Esc](#)[Print Version](#)[Interactive Discussion](#)

© EGU 2003

total reaction at 298 K and as high as 70% at lower temperatures (Hynes and Wine, 1996; Arsene et al., 1999). In the case of XO-initiated atmospheric DMS oxidation (X=Br, Cl), DMSO yield is expected to be around 100% (Barnes et al., 1991; Ingham et al., 1999). DMSO is also produced via multiphase reactions of DMS with O₃ (Lee and Zhu, 1994). To our knowledge the present gaseous DMSO measurements are the first to have been conducted in the Mediterranean area. DMSO ranges from below the detection limit (0.03 pmol·mol⁻¹) to 10.1 pmol·mol⁻¹ with a mean value of 1.7 pmol·mol⁻¹ (Fig. 3a). DMSO appeared to generally follow the DMS variability, especially during the first week of the campaign (28 July–3 August). However, using the full data sets no statistically significant correlation was found between these two compounds ($r^2=0.1$), reflecting different lifetime and removal pathways.

Very low DMSO levels (close to the detection limit) were observed between 6–12 August as well as during the end of the campaign. The low DMSO values at the end of the campaign were due to very low wind speed and consequently very low atmospheric DMS levels (Fig. 2a). The low DMSO values between 10–11 August, despite the relative high DMS levels can be attributed to high RH and aerosol surface during that period (Fig. 1). The above result could indicate a significant role of heterogeneous reactions in controlling the DMSO levels in agreement with the conclusions by Davis et al. (1998, 1999) and Sciare et al. (2001).

The observed DMSO levels fall between those reported by Putaud et al. (1999) for a Northern Atlantic coastal area (0.45 pmol·mol⁻¹) and by Sciare et al. (2000) during summertime at Amsterdam Island, situated in a similar latitude in the southern hemisphere. The DMSO values during MINOS are also lower than the values reported by Nowak et al. (2001; 4.5–11.5 pmol·mol⁻¹) over the tropical Pacific where the authors reported the possibility of an additional source of DMSO in the tropics.

The values reported for coastal Antarctica by Berresheim et al. (1998; 0.2–25 pmol·mol⁻¹) and Legrand et al. (2001; 0.4–57 pmol·mol⁻¹) are significantly higher than our data. A possible explanation is the lower temperature during these experiments that favour DMSO production through the addition channel of the OH-initiated

**Gaseous and
particulate sulfur
species**

H. Bardouki et al.

[Title Page](#)[Abstract](#)[Introduction](#)[Conclusions](#)[References](#)[Tables](#)[Figures](#)[◀](#)[▶](#)[◀](#)[▶](#)[Back](#)[Close](#)[Full Screen / Esc](#)[Print Version](#)[Interactive Discussion](#)

© EGU 2003

DMS reaction. Furthermore, Davis et al. (1998) showed that the elevated DMSO levels reported by Berresheim et al. (1998), were short-term spikes due to downward mixing of air from the middle troposphere enriched in DMSO compared to the ground. Therefore, these results suggested a change in DMSO chemistry and relative product yields with altitude. We have indication that similar situation occurred during MINOS. As in Berresheim et al. (1998), DMSO spikes seem to be associated with low dew point (Fig. 3b). However, clearly additional field BL and FT measurements of DMSO are needed in the Mediterranean area.

Figure 3c shows the diurnal variation of normalized DMSO during the MINOS experiment. Normalized DMSO shows a minimum around 14:00 (LT) as well as a maximum around 19:00 (LT). The DMSO minimum occurs almost simultaneously with the OH maximum and therefore, may be attributable to the relatively fast DMSO reaction with OH radicals (about 15 times faster than DMS+OH; Urbanski et al., 1998). The DMSO maximum at 19:00 coincides with the DMS maximum that may be explained by the very low levels of OH radicals. In addition at that time of the day low dew point is also observed, which also favors high DMSO levels. However, the existing data set does not allow a clear distinction between these two factors.

During nighttime, when DMS reacts with NO₃ radicals, DMSO levels are also decreasing and a decay rate of $3.5 \times 10^{-5} \text{ s}^{-1}$ was estimated from the data presented in Fig. 3b. Based on the rate constant of DMSO with NO₃ radicals of $(1.7 \pm 0.3) \times 10^{-13} \text{ cm}^3 \text{ molecule}^{-1} \text{ s}^{-1}$ and $(5 \pm 3.8) \times 10^{-13} \text{ cm}^3 \text{ molecule}^{-1} \text{ s}^{-1}$ (about 2–6 times slower than DMS+NO₃; Barnes et al., 1989; Falbe-Hansen et al., 2000) and the mean NO₃ levels of $10^8 \text{ molecule cm}^{-3}$ observed during the campaign (Vrekoussis et al., 2003), a decay rate of $(1.7–5) \times 10^{-5} \text{ s}^{-1}$ is estimated. Thus without neglecting possible dilution of DMSO by the land-breeze situation, the DMSO decrease during night could be mainly explained by reaction with NO₃ radicals.

3.3. MS⁻

MS⁻ in the aerosol phase (Fig. 4a) ranges between 1.1 and 37.5 pmol·mol⁻¹ (mean value of 11.5 pmol·mol⁻¹) within the range of summertime values reported for the area (Kouvarakis and Mihalopoulos, 2002; Kubilay et al., 2002). During the campaign the mean DMS/MS⁻ ratio was 2.5, close to the value of 3 reported by Mihalopoulos et al. (1992) for summertime measurements at a coastal area in French Brittany under continental influence. These values are, however, significantly lower than those reported for the remote marine atmosphere by Ayers et al. (1995; ratio approximately 8 at Cape Grim) and by Wylie and de Mora (1996; ratio ranging from 8–13 in New Zealand). According to laboratory experiments by Yin et al. (1990) and Patroescu et al. (1999), the low DMS/MS⁻ ratios observed during the campaign could indicate that the oxidation of DMS to MSA under the high NO_x regime during MINOS was more efficient compared to the remote marine conditions.

Of particular interest is the relation of MS⁻ with DMSO during MINOS. Davis et al. (1998, 1999) proposed that heterogeneous reactions of DMSO can account for a significant part of the observed MS⁻. During the periods with high RH associated in most times with high aerosol surface (in particular, 5 August and 14–18 August) DMSO significantly correlated with MS⁻ (DMSO/MS⁻ slope=0.3, r²=0.5, p<0.05). On the other hand, during periods with low RH and low aerosol surface (7 and 22 August) the slope becomes smaller by a factor of 8–20, probably indicating much lower production of MS⁻ via multiphase reactions.

Figure 4b presents the diurnal variation of normalized MS⁻ during the campaign. Similar to DMS and DMSO, MS⁻ presents a clear maximum in the evening. From the data presented in Fig. 4b a decay rate of 7.9×10⁻⁶ s⁻¹ was estimated for MS⁻ during nighttime. This value is very close to the value of 6.6×10⁻⁶ s⁻¹ estimated by Huebert et al. (1996), in the equatorial Pacific marine boundary layer during the same period of the year, under clean conditions. These authors attributed the nighttime decrease of MS⁻ by dry deposition and entrainment velocity from the free troposphere. The good

Title Page

Abstract

Introduction

Conclusions

References

Tables

Figures

◀

▶

◀

▶

Back

Close

Full Screen / Esc

Print Version

Interactive Discussion

agreement between the two data sets obtained under clean and semi-polluted marine conditions, indicates that despite the important reaction of DMS with NO_3 during night-time, MS^- is not expected to be an important oxidation product of the NO_3 initiated oxidation of DMS in the atmosphere and that this reaction is expected to lead mainly to SO_2 via the initial production of CH_3SCH_2 which is identical to the first intermediate sulfur species produced in the DMS+OH abstraction channel (Kanakidou et al. 2003).

3.4. SO_2 and nss-SO_4^{2-}

SO_2 ranged between 220 and 2970 $\text{pmol}\cdot\text{mol}^{-1}$ (mean of 1030 $\text{pmol}\cdot\text{mol}^{-1}$; Fig. 5). Nss-SO_4^{2-} (calculated using Na^+ as a seasalt tracer) ranged between 330 and 7100 $\text{pmol}\cdot\text{mol}^{-1}$ (mean of 1440 $\text{pmol}\cdot\text{mol}^{-1}$) (Fig. 5). SO_2 and nss-SO_4^{2-} levels are in agreement with the summertime values reported for Crete (Kouvarakis and Mihalopoulos, 2002; Sciare et al., 2003). Both SO_2 and nss-SO_4^{2-} significantly correlated ($r^2=0.79$ and 0.81, respectively) with total SO_x (sum of $\text{nss-SO}_4^{2-} + \text{SO}_2$) with slopes of 0.48 and 0.52, respectively, indicative of aged air masses (Luria et al. 1996; Sciare et al., 2003). Based on a source receptor model, Sciare et al. (2003) concluded that the majority of SO_2 and nss-SO_4^{2-} in the area originates from long-range transport from anthropogenic sources in central and E. Europe.

3.5. H_2SO_4

In the following paragraph the contribution of H_2SO_4 to the levels of particulate nss-SO_4^{2-} is discussed. Figure 6 shows the H_2SO_4 measurements for the whole campaign. H_2SO_4 ranged between the detection limit of $<1\times 10^5$ and 9.0×10^7 molecules cm^{-3} (mean value= 1.0×10^7 molecules cm^{-3}). These values are by almost a factor of 10 higher than those reported for remote marine environments in earlier studies (1.6×10^6 molecules cm^{-3} : Jefferson et al., 1998; 1.5×10^6 molecules cm^{-3} : Berresheim et al., 2002). Meteorological factors such as relative humidity and dew point, and

[Title Page](#)[Abstract](#)[Introduction](#)[Conclusions](#)[References](#)[Tables](#)[Figures](#)[◀](#)[▶](#)[◀](#)[▶](#)[Back](#)[Close](#)[Full Screen / Esc](#)[Print Version](#)[Interactive Discussion](#)

© EGU 2003

**Gaseous and
particulate sulfur
species**

H. Bardouki et al.

[Title Page](#)
[Abstract](#)
[Introduction](#)
[Conclusions](#)
[References](#)
[Tables](#)
[Figures](#)
[◀](#)
[▶](#)
[◀](#)
[▶](#)
[Back](#)
[Close](#)
[Full Screen / Esc](#)
[Print Version](#)
[Interactive Discussion](#)

© EGU 2003

physicochemical parameters like aerosol surface have been reported as important factors controlling the variation of gaseous H_2SO_4 levels. Although the highest H_2SO_4 levels were observed during periods with low RH and dew point (Fig. 6) no statistically significant correlation was observed between the H_2SO_4 data and these parameters when the data is analysed for the entire measurement period.

Figure 7a presents the hourly mean variation of H_2SO_4 during the campaign in conjunction with corresponding hourly mean OH values (averaged from the 5 min time-integrated data presented by Berresheim et al., 2003). The diurnal profile of H_2SO_4 follows quite well that of OH radicals indicating a clear photochemical origin for H_2SO_4 , i.e. via the reaction of gaseous SO_2 with OH radicals. The same tendency is observed when the comparison between H_2SO_4 and OH is performed on a daily-average basis. This is clearly seen in Fig. 7b demonstrating an important correlation between the normalized hourly average values of H_2SO_4 and OH for the whole campaign (slope=0.85, $r^2=0.87$).

To better understand the fate of H_2SO_4 , we can assume that H_2SO_4 was in steady state conditions with its precursor SO_2 . Under this assumption the reaction of $\text{SO}_2 + \text{OH}$ radicals is considered as the only source of H_2SO_4 and condensation (of H_2SO_4) onto the existing aerosol surface as the only sink:

$$k[\text{SO}_2][\text{OH}] = k_{\text{cs}}[\text{H}_2\text{SO}_4] \quad (1)$$

where $k = 8.5 \times 10^{-13} \text{ cm}^3 \text{ molecule}^{-1} \text{ s}^{-1}$ at 298 K (DeMore et al., 1997) and k_{cs} the pseudo-first order rate constant for the H_2SO_4 condensational sink that can be calculated from the Fuchs-Sutugin equation including the sticking coefficient and the aerosol surface concentration (Fuchs and Sutugin, 1970). The OH and H_2SO_4 concentrations were averaged over 2–3 h corresponding to the time-averaged measurements of SO_2 . Thus, by plotting the H_2SO_4 production rate by SO_2 reaction with OH radicals ($k [\text{SO}_2][\text{OH}]$) as a function of $[\text{H}_2\text{SO}_4]$, a significant correlation was obtained on a daily basis (Table 2 and Fig. 8) and when all the 2–3 hourly data are plotted together (Fig. 8). Regression slopes correspond to k_{cs} ranging between 0.0071 s^{-1} and 0.0167 s^{-1} (mean

**Gaseous and
particulate sulfur
species**

H. Bardouki et al.

[Title Page](#)
[Abstract](#)
[Introduction](#)
[Conclusions](#)
[References](#)
[Tables](#)
[Figures](#)
[◀](#)
[▶](#)
[◀](#)
[▶](#)
[Back](#)
[Close](#)
[Full Screen / Esc](#)
[Print Version](#)
[Interactive Discussion](#)

© EGU 2003

value of 0.011 s^{-1}) during the experiment. It is interesting to note that the daily averaged k_{cs} values follows remarkably the variation of RH ($r^2=0.6$, data not shown), indicating shorter lifetime under increased RH conditions, probably due to hygroscopic aerosol growth and thus increased aerosol surface (Fig. 1). The very short lifetime for H_2SO_4 (1–2.5 min) is in agreement with the assumption of steady state condition between production and loss to particles and consistent with the good correlation between OH and H_2SO_4 shown above.

Based on the k_{cs} values derived from the regression analysis, the surface aerosol data, and the use of the Fuchs-Sutugin equation, the mass accommodation coefficient “ α ” can be calculated for H_2SO_4 at a mean temperature during MINOS of 300 K. The calculated mean value of 0.52 ± 0.28 (geometric mean of 0.49) is in excellent agreement with the value of 0.5 derived by Jefferson et al. (1997) at 298 K on the basis of laboratory experiments. The use of an accommodation coefficient of 0.5 is supported by field studies of H_2SO_4 production and loss (Eisele and Tanner, 1993) and model results of aerosols nucleation and growth (Kerminen and Wexler, 1995).

The above data set can be used to investigate whether the observed H_2SO_4 levels can account for the observed levels of particulate nss-SO_4^{2-} . From mass transfer considerations the aerosol sulphate concentration derived from condensation of gas phase H_2SO_4 on to the aerosol surface can be estimated by the following equation:

$$\text{nss-SO}_4^{2-} = k_{csl} [\text{H}_2\text{SO}_4] \Delta t \quad (2)$$

By using mean values of $1.2 \times 10^{-2} \text{ s}^{-1}$ and $10^7 \text{ molecules cm}^{-3}$ for k_{cs} and H_2SO_4 respectively, the time needed to produce measured nss-SO_4^{2-} levels of $1.4 \text{ nmol} \cdot \text{mol}^{-1}$ is 3.5 days, which falls within the range of estimated residence times of submicronic aerosols in the marine boundary layer. Thus condensational uptake of H_2SO_4 could dominate nss-SO_4^{2-} formation in the Mediterranean area at some distance from major industrial sources with direct nss-SO_4^{2-} emissions. In addition, heterogeneous reaction of SO_2 on aerosol surface might also significantly contribute.

3.6. MSA(g)

Figure 9 shows the results of the gas phase MSA measurements for the whole campaign. MSA ranged from below the detection limit (3×10^4 molecules cm^{-3}) to 3.7×10^7 molecules cm^{-3} . The average value recorded during the campaign (5.2×10^5 molecules cm^{-3}) is slightly lower than those recorded during previous studies (9.5×10^5 molecules cm^{-3} : Jefferson et al., 1998; 1.2×10^6 molecules cm^{-3} : Berresheim et al., 2002). However these studies have been conducted under significantly lower temperatures, and laboratory experiments (Arsene et al., 1999) have shown that temperature significantly influences the MSA yields from DMS oxidation.

MSA appears to be more sensitive than H_2SO_4 to variations of RH, dew point and aerosol surface, probably due to its higher vapor pressure (Kreidenweis and Seinfeld, 1988, Berresheim et al., 2002). This is clearly seen in Figs. 9a,b, presenting the variation of MSA and RH during the experiment (Fig. 9a) as well as the regression between these two parameters (Fig. 9b; $r^2=0.23$, $p<0.001$). Similar relations with RH have been observed when MSA is also plotted against aerosol surface. MSA clearly decreases with increasing RH, dew point and aerosol surface. Especially all the significant elevations in MSA concentration occur under low RH (smaller than 30%), in agreement with the observations over the equatorial Pacific by Mauldin et al. (1999) or on the western coast of Ireland at Mace Head (Berresheim et al., 2002). When compared to H_2SO_4 the different behavior can be explained by the higher vapor pressure of MSA (Kreidenweis and Seinfeld, 1988). The larger volatility of MSA compared to H_2SO_4 can be also seen in Fig. 10, presenting the variation of MSA and MS^- during the experiment. An inverse correlation can be seen between gaseous and particulate MSA levels. Especially at low RH the partitioning is such that the MSA resides mainly in the gas phase. Conversely, at high RH values most of the MS^- exists in particulate form.

Figures 11a,b present two well distinguished cases of diurnal variation of MSA during the campaign: In the first, MSA (Fig. 11a) follows closely the OH variation, as in the case of H_2SO_4 . In the second in addition to the MSA peak occurring in conjunction

Title Page

Abstract

Introduction

Conclusions

References

Tables

Figures

◀

▶

◀

▶

Back

Close

Full Screen / Esc

Print Version

Interactive Discussion

**Gaseous and
particulate sulfur
species**

H. Bardouki et al.

with OH, several secondary peaks also can be distinguished (Fig. 11b). A closer look of these cases demonstrates that the first type of profile with a single maximum occurred mainly under periods with high RH (14–18 August). The covariation of MSA with OH radicals indicates a clear photochemical origin of MSA, i.e., possibly via the reaction of gaseous DMS, its precursor, with OH radicals. The MSA peaks observed in the second type of profile coincide with periods of low RH or dew point and are in very good agreement with the general tendency of MSA relative to RH observed during the entire campaign.

The above data set and the simultaneous measurements of DMS, gaseous MSA and particulate MS^- offer a unique opportunity to estimate the yield (Y) of MSA from the OH initiated oxidation of DMS. Laboratory experiments showed that this yield is highly dependant on NO_x and can range from less than a few percents (Patroescu et al., 1999) to values as high as 50% (Hatakeyama et al., 1982). For this purpose, we assume that MSA is in steady state conditions with its precursor DMS. Under this assumption the reaction of DMS+OH radicals is considered as the only source of MSA, while condensation onto the existing aerosol surface is the only sink for MSA:

$$k[DMS][OH][Y]=k_{cs}[MSA] \quad (3)$$

where $KOH+DMS$ is taken from Hynes et al. (1986) and k_{cs} is the pseudo-first order rate constant for the MSA condensational sink and is derived using two different approaches. The first using the Fuchs-Sutugin equation (Fuchs and Sutugin, 1970) and the second using the k_{cs} derived from H_2SO_4 but corrected using an accommodation coefficient “ α ” for MSA equal to 0.075 (De Bruyn et al., 1994) at $T=300$ K). The second approach is used since aerosol surface data are not available for the whole period. Table 3 presents the MSA yield as well as the correlation coefficient estimated by applying the above Eq. (3) for each day.

A quite good agreement was found in the MSA yield using these approaches. Statistically significant correlations were observed only during days with no important changes in RH or dew point, since both parameters can influence the MSA levels.

[Title Page](#)[Abstract](#)[Introduction](#)[Conclusions](#)[References](#)[Tables](#)[Figures](#)[◀](#)[▶](#)[◀](#)[▶](#)[Back](#)[Close](#)[Full Screen / Esc](#)[Print Version](#)[Interactive Discussion](#)

**Gaseous and
particulate sulfur
species**

H. Bardouki et al.

By considering only the periods with statistically significant correlation coefficients (r^2), the calculated MSA yield is very low and ranges between (10^{-3} to 4.2×10^{-3} , mean of 1.9×10^{-3}), but it is in good agreement with the value of 5×10^{-3} deduced by Davis et al. (1999) for the equatorial Pacific boundary layer.

To investigate whether the observed MSA levels can account for the observed particulate levels MS^- , as in the case of H_2SO_4 , by assuming mass transfer considerations, the MS^- levels from condensation of MSA on to the aerosol surface can be derived by the following equation:

$$MS^- = k_{cs}[MSA]\Delta t \quad (4)$$

Given the very important variability of MSA as a function of RH we have considered two different cases: 1) the days with particularly low RH (7 and 21–22 August) and 2) the rest of the campaign.

For the first case, the time needed to reproduce the measured MS^- levels range from 16 h on 7 August to 2.6 days for the period 21–22 August. These lifetimes fall within the range of residence time of submicronic aerosols in the marine boundary layer, indicating that the measured MS^- levels are in equilibrium with the corresponding gas phase MSA.

For the remaining part of the campaign, the time needed to reproduce the measured MS^- levels has been calculated to be around 19 days, period significantly higher than the residence time of submicronic aerosols. Thus gaseous to particle conversion of MSA can not account for the observed levels of MS^- . The above results are in agreement with those of Davis et al. (1998, 1999) who proposed that multiphase reactions involving DMSO can account for the observed MS^- levels. Bardouki et al. (2002) conducted aqueous phase experiments and reported that DMSO reacts very fast with OH radicals leading to MS^- formation with almost 100% yield.

By using the DMSO concentrations observed during the campaign the production rate of MS^- via multiphase reactions can account for the measured MS^- levels. Details on these calculations can be found in Kanakidou et al. (2003).

[Title Page](#)[Abstract](#)[Introduction](#)[Conclusions](#)[References](#)[Tables](#)[Figures](#)[◀](#)[▶](#)[◀](#)[▶](#)[Back](#)[Close](#)[Full Screen / Esc](#)[Print Version](#)[Interactive Discussion](#)

© EGU 2003

3.7. Conclusions-Implications for the S cycle in the area

During the MINOS campaign conducted in July–August 2001 in a coastal location in Crete, measurements of DMS and its major gas and aerosol phase oxidation products as well as the dominant radical species (OH and NO₃) involved in DMS oxidation have been performed. The analysis of this extensive data set shows that:

1. DMS variability during the MINOS campaign in the coastal area of Crete was mainly governed by NO₃ radicals and air mass origin. DMS presents a clear night-time minimum and thus DMS diurnal variation is opposite to that observed in the remote marine atmosphere of the southern hemisphere.
2. A very short lifetime has been calculated for H₂SO₄ (1–2 min) with respect to condensation on the existing aerosol surface (k_{cs}). Based on the calculated k_{cs} , the surface aerosol data and the use of the Fuchs-Sutugin equation, the average mass accommodation coefficient “ α ” for H₂SO₄ at 300 K was calculated to be 0.52 ± 0.28 . Finally, condensational uptake of H₂SO₄ is proved to play a very important role in the nss-SO₄²⁻ budget over the study area.
3. MSA seems to be very sensitive to variations of RH, dew point and aerosol surface compared to H₂SO₄. This can be explained by the higher vapor pressure of MSA compared to H₂SO₄. From the simultaneous measurements of DMS, gaseous MSA and OH radicals, a MSA yield from the OH-initiated oxidation of DMS can be calculated, which ranges between 10^{-3} and 4.2×10^{-3} (mean of 1.9×10^{-3}) representing the lowest values reported so far in the literature. These values should be considered as upper limits since laboratory work clearly shows enhancement of MSA yield in the presence of NO_x as in our case.
4. With the exception of the periods with low RH, gas to particle conversion of MSA can not account for the observed levels of MS⁻. This result is consistent with the observations by Davis et al. (1998,1999) based on two campaigns performed in

Title Page

Abstract

Introduction

Conclusions

References

Tables

Figures

◀

▶

◀

▶

Back

Close

Full Screen / Esc

Print Version

Interactive Discussion

**Gaseous and
particulate sulfur
species**

H. Bardouki et al.

[Title Page](#)[Abstract](#)[Introduction](#)[Conclusions](#)[References](#)[Tables](#)[Figures](#)[⏪](#)[⏩](#)[◀](#)[▶](#)[Back](#)[Close](#)[Full Screen / Esc](#)[Print Version](#)[Interactive Discussion](#)

© EGU 2003

Antarctica and equatorial Pacific. Given the completely different conditions under which these three experiments have been performed, the above results indicate that under humidity conditions typical of the marine boundary layer (RH higher than 40%), multiphase reactions involving DMSO could account for the observed MS⁻ levels. These reactions should be taken into account in any attempt to model the biogenic sulfur cycle.

Acknowledgement. This program was funded by the EC Programme El-Cid, n° ENVK2-CT-1999-00033. H. Berresheim thanks J. Lelieveld for the opportunity to participate in MINOS, M. de Reus and the MPI and ECPL teams for logistical help, and T. Elste and G. Stange for their assistance in carrying out the H₂SO₄ and MSA measurements. The DWD work was financially supported by the Max-Planck-Society (MPG) and the German Weather Service (DWD/BMVBW).

References

- Andreae, M. O., Ferek, R. J., Bermond, F., Byrd, K. P., Engstrom, R. T., Hardin, S., Houmère, D., LeMarrec, F., Raemdonck, H., and Chatfield, R. B.: Dimethylsulfide in the marine atmosphere. *J. Geophys. Res.*, 90 (12), 891–900, 1985.
- Arsene, C., Barnes, I., and Becker, K. H.: FT-IR product study of the photooxidation of dimethyl sulphide: temperature and O₂ partial pressure dependence. *Physical Chemistry and Chemical Physics* 1, 5463–5470, 1999.
- Ayers, G. P., Bentley, S. T., Ivey, J. P., and Forgan, B. W.: Dimethylsulfide in marine air at Cape Grim, 411S. *J. Geophys. Res.*, 100, 21 013–21 021, 1995.
- Baboukas, E. D., Kanakidou, M., and Mihalopoulos, N.: Carboxylic acids in gas and particulate phase above the Atlantic ocean, *J. Geophys. Res.*, 105, 14 459–14 471, 2000.
- Bardouki, H., Barcellos da Rosa, M., Mihalopoulos, N., Palm, W.-U., and Zetzsch, C.: Kinetics and mechanism of the oxidation of dimethylsulfoxide (DMSO) and methanesulfinat (MSI⁻) by OH radicals in aqueous medium, *Atmos. Environ.*, 36, 4627–4634, 2002.
- Barnes, I., Bastian, V., Becker, K. H., and Martin, D.: Fourier Transform IR studies of the reactions of dimethyl sulfoxide with OH, NO₃ and Cl radicals, in: *Biogenic Sulfur in the*

Environment, Salzmann, E. S., Cooper, W. J. (Eds), ACS Symposium Series 393, pp. 476, 488, 1989.

Barnes, I., Bastian, V., Becker, K. H., and Overath, R.: Kinetic study of the reactions of IO, BrO, ClO with dimethylsulfide, *International Journal of Chemical Kinetics*, 23, 579–591, 1991.

5 Berresheim, H. and Eisele, F. L.: Sulfur Chemistry in the Antarctic Troposphere Experiment: An overview of project SCATE, *J. Geophys. Res.*, 103 D1, 1619–1627, 1998.

Berresheim, H., Huey, J. W., Thorn, R. P., Eisele, F. L., Tanner, D. J., and Jefferson, A.: Measurements of dimethyl sulfide, dimethyl sulfoxide, dimethyl sulfone, and aerosol ions at Palmer Station, Antarctica, *J. Geophys. Res.*, 103, 1629–1637, 1998.

10 Berresheim, H., Elste, T., Tremmel, H. G., Allen, A. G., Hansson, H., Rosman, K., DalMaso, M., Mäkelä, J. M., Kulmala, M., and O'Dowd, C.: Gas-aerosol relationships of OH, H₂SO₄ and MSA: Observations in the coastal marine boundary layer at Mace Head, Ireland. *J. Geophys. Res.*, 107, no 8100, doi:10.1029/2000JD000229, 2002.

Berresheim, H., Plass-Dülmer, C., Elste, T., Mihalopoulos, N., and Rohrer, F.: OH in the coastal boundary layer of Crete during MINOS: Measurements and relationship with ozone photolysis, *Atmos. Chem. Phys.*, 3, 639–649, 2003.

Berresheim, H., Elste, T., Plass-Duelmer, C., Eisele, F. L., and Tanner, D. J.: Chemical ionization mass spectrometer for long-term measurements of atmospheric OH and H₂SO₄, *Int. J. Mass Spectrom.*, 202, 91–109, 2000.

20 Berresheim, H., Wine, P., and Davis, D.: Sulfur in the atmosphere, in *Composition Chemistry and climate of the Atmosphere*, Singh, H. B. (Ed), Van Nostrand Reinhold, New York, 251–307, 1995.

Charlson, R. J., Lovelock, J. E., Andreae, M. O., and Warren, S. G.: Oceanic phytoplankton, atmospheric sulphur, cloud albedo and climate, *Nature*, 326, 655–661, 1987.

25 Cofer, W. R., Collins, V. G., and Talbot, R.: Improved aqueous scrubber for collection of soluble atmospheric trace gases, *Environ. Sci. Technol.*, 19, 557–560, 1985.

Davis, D., Chen, G., Bandy, A., Thornton, D., Eisele, F., Mauldin, L., Tanner, D., Lenschow, D., Fuelberg, H., Huebert, B., Heath, J., Clarke, A., and Blake, D.: Dimethyl sulfide oxidation in the equatorial Pacific: Comparison of model simulations with field observations for DMS, SO₂, H₂SO₄(g), MSA(g), and MS, and NSS, *J. Geophys. Res.*, 104, 5765–5784, 1999.

30 Davis, D., Chen, G., Kasibhatla, P., Jefferson, A., Tanner, D., Eisele, F., Lenschow, D., Neff, W., and Berresheim, H.: DMS oxidation in the Antarctic marine boundary layer: Comparison of model simulations and field observations of DMS, DMSO, DMSO₂, H₂SO₄(g), MSA(g), and

**Gaseous and
particulate sulfur
species**

H. Bardouki et al.

Title Page

Abstract

Introduction

Conclusions

References

Tables

Figures

◀

▶

◀

▶

Back

Close

Full Screen / Esc

Print Version

Interactive Discussion

**Gaseous and
particulate sulfur
species**H. Bardouki et al.

[Title Page](#)[Abstract](#)[Introduction](#)[Conclusions](#)[References](#)[Tables](#)[Figures](#)[◀](#)[▶](#)[◀](#)[▶](#)[Back](#)[Close](#)[Full Screen / Esc](#)[Print Version](#)[Interactive Discussion](#)

© EGU 2003

MSA(p), *J. Geophys. Res.*, 103, 1657–1678, 1998.

De Bruyn, W. J., Shorter, J. A., Davidovits, P., Worsnop, D. R., Zahniser, M. S., and Kolb, C. E.: Uptake of gas phase sulfur species methanesulfonic acid, dimethylsulfoxide, and dimethyl sulfone by aqueous surfaces, *J. Geophys. Res.*, 99 D8, 16 927–16 932, 1994.

5 DeMore, W. B., Sander, S. P., Golden, D. M., Hampson, R. F., Kurylo, M. J., Howard, C. J., Ravishankara, A. R., Kolb, C. E., and Molina, M. J.: Chemical kinetics and photochemical data for use in stratospheric modeling, *JPL Publ.*, 97-4, 1997.

Eisele, F. L. and Tanner, D. J.: Measurement of the gas phase concentration of H₂SO₄ and methane sulfonic acid and estimates of H₂SO₄ production and loss in the atmosphere, *J.*
10 *Geophys. Res.*, 98, 9001–9010, 1993.

Falbe-Hansen, H., Sorensen, S., Jensen, N. R., Pedersen, T., and Hjorth, J.: Atmospheric gas-phase reactions of dimethylsulphoxide and dimethylsulphone with OH and NO₃ radicals, Cl atoms and ozone, *Atmos. Environ.*, 34, 1543–1551, 2000.

Fuchs, N. and Sutugin, A. G.: *Highly Dispersed Aerosols*, Butterworth-Heinemann, Newton, Mass., 47–60, 1970.

15 Ganor, E., Foner, H. A., Bingemer, H. G., Udusti, R., and Setter, I.: Biogenic sulphate generation in the Mediterranean Sea and its contribution to the sulphate anomaly in the aerosol over Israel and in the Eastern Mediterranean, *Atmos. Environ.*, 34, 3453–3462, 2000.

Hatakeyama, S., Okuda, M., and Akimoto, H.: Formation of sulfur dioxide and methanesulfonic acid in the photooxidation of dimethyl disulfide in air, *Geophys. Res. Lett.*, 9, 583–586, 1982.

20 Huebert, B. J., Wylie, D. J., Zhuang, L., and Heath, J.A.: Production and loss of methanesulfonate and non-sea salt sulfate in the equatorial Pacific marine boundary layer, *Geophys. Res. Lett.*, 23, 7, 737–740, 1996.

Hynes, A. J. and Wine, P. H.: The atmospheric chemistry of dimethylsulfoxide (DMSO) kinetics and mechanism of the OH+DMSO reaction, *J. Atmos. Chem.*, 24, 23–37, 1996.

25 Hynes, A. J., Wine, P. H., and Semmes, D. H.: Kinetics and mechanisms of OH reactions with organic sulfides, *J. Phys. Chem.*, 90, 4148–4156, 1986.

Ingham, T., Bauer, D., Sander, R., Crutzen, P. J., and Crowley, J. N.: Kinetics and Products of the Reactions BrO+DMS and Br+DMS at 298 K, *J. Phys. Chem. A.*, 103, 7199–7209, 1999.

30 IPCC, *Climate Change 2001: The scientific basis*, Summary for policy makers and technical summary of the working group 1 report, edited by Watson, R., et al., Cambridge University Press, Cambridge, 98p, 2001.

Jefferson, A., Tanner, D. J., Eisele, F. L., Davis, D. D., Chen, G., Crawford, J., Huey, J. W.,

**Gaseous and
particulate sulfur
species**

H. Bardouki et al.

[Title Page](#)[Abstract](#)[Introduction](#)[Conclusions](#)[References](#)[Tables](#)[Figures](#)[◀](#)[▶](#)[◀](#)[▶](#)[Back](#)[Close](#)[Full Screen / Esc](#)[Print Version](#)[Interactive Discussion](#)

© EGU 2003

Torres, A. L., and Berresheim, H.: OH photochemistry and methane sulfinic formation in the coastal Antarctic boundary layer, *J. Geophys. Res.*, 103 D1, 1647–1656, 1998.

Jefferson, A., Eisele, F. L., Ziemann, P. Z., Marti, J. J., Weber, R. J., and McMurry, P.: Measurements of the H_2SO_4 mass accommodation coefficient onto polydisperse aerosol, *J. Geophys. Res.*, 102, 19 021–19 028, 1997.

Kanakidou, M., Vrekoussis, M., Berresheim, H., Bardouki, H., Sciare, J., Kouvarakis, G., Economou, C., and Mihalopoulos, N.: Gaseous (DMS, MSA, SO_2 , H_2SO_4 and DMSO) and particulate (sulfate and methanesulfonate) sulfur species during the MINOS campaign: 2. A Modelling approach, *ACP*, this issue (in preparation).

Kerminen, V. and Wexler, A. S.: Enhanced formation and development of sulfate particles due to marine boundary layer circulation, *J. Geophys. Res.*, 100, 23 051–23 062, 1995.

Kouvarakis, G., Tsigaridis, K., Kanakidou, M., and Mihalopoulos, N.: Temporal variations of surface regional background ozone over Crete Island in southeast Mediterranean, *J. Geophys. Res.*, 105, 4399–4407, 2000.

Kouvarakis, G. and Mihalopoulos, N.: Seasonal variation of dimethylsulfide in the gas phase and of methanesulfonate and non-sea-salt sulfate in the aerosol phase measured in the eastern Mediterranean atmosphere, *Atmos. Environ.*, 36, 6, 929–938, 2002.

Kouvarakis, G., Bardouki, H., and Mihalopoulos, N.: Sulfur budget above the Eastern Mediterranean: relative contribution of anthropogenic and biogenic sources, *Tellus*, 54, 201–213, 2002.

Kreidenweiss, S. M. and Seinfeld, J. H.: Nucleation of sulfuric acid water and methansulfonic acid water particles: Implications for the atmospheric chemistry of organic species, *Atmos. Environ.*, 22, 283–296, 1988.

Kubilay, N., Kocak, M., Cokacar, T., Oguz, T., Kouvarakis, G., and Mihalopoulos, N.: Influence of Black Sea and local biogenic activity on the seasonal variation of aerosol sulfur species in the eastern Mediterranean atmosphere, *Glob. Biogeochem. Cycl.*, 16, NO. 4, 1079, doi:10.1029/2002GB001880, 2002.

Lee, Y. and Zhu, X.: Aqueous reaction kinetics of ozone and dimethylsulfide and its atmospheric implications, *J. Geophys. Res.*, 99, 3597–3605, 1994.

Legrand, M., Sciare, J., Jourdain, B., and Genthon, C.: Subdaily variations of atmospheric dimethylsulfide, dimethylsulfoxide, methanesulfonate, and non-sea-salt sulfate aerosols in the atmospheric boundary layer at Dumont d'Urville (coastal Antarctica) during summer, *J. Geophys. Res.*, 106 D13, 14 409–14 422, 2001.

**Gaseous and
particulate sulfur
species**H. Bardouki et al.

[Title Page](#)[Abstract](#)[Introduction](#)[Conclusions](#)[References](#)[Tables](#)[Figures](#)[◀](#)[▶](#)[◀](#)[▶](#)[Back](#)[Close](#)[Full Screen / Esc](#)[Print Version](#)[Interactive Discussion](#)

© EGU 2003

- Liss, P. S. and Merlivat, L.: The Role of Air-Sea Exchange in Geochemical Cycling edited by P. Buat-Ménard, Dordrecht, D. Reidel Pub. Co., 113–127, 1986.
- Luria, M., Peleg, M., Sharf, G., Siman tov-Alper, D., Spitz, N., Ben Ami, Y., Gawii, Z., Lifschitz, B., Yitzchaki, A., and Seter, I.: Atmospheric sulfur over the eastern Mediterranean region, *J. Geophys. Res.*, 101, 25 917–25 930, 1996.
- Mauldin III, R. L., Tanner, D. J., Heath, J. A., Huebert, B. J., and Eisele, F. L.: Observations of H₂SO₄ and MSA during PEM-Tropics-A, *J. Geophys. Res.*, 104 D5, 5801–5816, 1999.
- Mihalopoulos, N., Stephanou, E., Kanakidou, M., Pilitsidis, S., and Bousquet, P.: Tropospheric aerosol ionic composition above the Eastern Mediterranean Area, *Tellus B*, 314–326, 1997.
- Mihalopoulos, N., Nguyen, B. C., Boissard, C., Campin, J. M., Putaud, J. P., Belviso, S., Barnes, I., and Becker, K. H.: Field study of dimethylsulfide oxidation in the boundary layer: variations of dimethylsulfide, methanesulfonic acid, sulfur dioxide, non sea salt sulfate and Aitken nuclei at a coastal site, *J. Atmos. Chem.*, 14, 459–477, 1992.
- Nguyen, B. C., Mihalopoulos, N., and Belviso, S.: Seasonal variation of atmospheric dimethylsulfide at Amsterdam island in the Southern Indian Ocean, *J. Atmos. Chem.*, 11, 123–143, 1990.
- Nowak, J. B., Davis, D., Chen, G., Eisele, F. L., Mauldin, R. L., Tanner, D. J., Cantrell, C., Kosciuch, E., Bandy, A., Thornton, D., and Clarke, A.: Airborne observations of DMSO, DMS, and OH at marine tropical latitudes, *Geophys. Res. Lett.*, 28(11), 2201–2204, 2001.
- Patroescu, J., Barnes, I., Becker, K. H., and Mihalopoulos, N.: FTIR product study of the OH initiated oxidation of DMS in the presence of NO_x, *Atmos. Environ.*, 33, 25–35, 1999.
- Putaud, J. P., Davison, B. M., Watts, S. F., Mihalopoulos, N., Nguyen, B. C., and Hewitt, C. N.: Dimethylsulfide and its oxidation products at two sites in Brittany (France), *Atmos. Environ.*, 33, 647–659, 1999.
- Schneider, J., Borrmann, S., Wollny, A. G., Bläsner, M., Mihalopoulos, N., Bardouki, H., Oikonomou, K., Sciare, J., Teller, A., and Levin, Z.: On-line mass spectrometric aerosol measurements during the MINOS campaign (Crete, August 2001) to be submitted to ACP, 2003.
- Sciare, J. and Mihalopoulos, N.: A new technique for sampling and analysis of atmospheric dimethylsulfoxide (DMSO), *Atmos. Environ.*, 34, 151–156, 2000.
- Sciare, J., Baboukas, E., and Mihalopoulos, N.: Short-term variability of atmospheric DMS and its oxidation products at Amsterdam Island during summer time, *J. Atmos. Chem.*, 39, 281–302, 2001.

**Gaseous and
particulate sulfur
species**

H. Bardouki et al.

[Title Page](#)[Abstract](#)[Introduction](#)[Conclusions](#)[References](#)[Tables](#)[Figures](#)[◀](#)[▶](#)[◀](#)[▶](#)[Back](#)[Close](#)[Full Screen / Esc](#)[Print Version](#)[Interactive Discussion](#)

© EGU 2003

Sciare, J., Bardouki, H., Moulin, C., and Mihalopoulos, N.: Aerosol sources and their contribution to the chemical composition of aerosols in the Eastern Mediterranean Sea during summertime, *Atmos. Chem. Phys.*, 3, 291–302, 2003.

Sciare, J., Kanakidou, M., and Mihalopoulos, N.: Diurnal and seasonal variation of atmospheric dimethylsulfoxide (DMSO) at Amsterdam Island in the southern Indian Ocean. *J. Geophys. Res.*, 105, 17 257–17 265, 2000.

Tanner, D. J., Jefferson, A., and Eisele, F. L.: Selected ion chemical ionization mass spectrometric measurement of OH, *J. Geophys. Res.*, 102, 6415–6425, 1997.

Urbanski, S. P., Stickel, R. E., and Wine, P.H.: Mechanistic and kinetic study of the gas-phase reaction of hydroxyl radical with dimethyl sulfoxide, *J. Phys. Chem.*, 102, 10 522–10 529, 1998.

Vrekoussis, M., Kanakidou, M., Mihalopoulos, N., Crutzen, P. J., Lelieveld, J., Perner, D., Berresheim, H., and Baboukas, E.: Role of NO₃ radicals in oxidation processes in the Eastern Mediterranean troposphere during the MINOS campaign, *Atmos. Chem. Phys. Discuss.*, 3, 3135–3169, 2003.

Watts, S. F., Brimblecombe, P., and Watson, A.: Methanesulphonic acid, dimethylsulfoxide and dimethyl sulphone in aerosols, *Atmos. Environ.*, 24, 353–359, 1990.

Wylie, D. and de Mora, S.: Atmospheric dimethylsulfide and sulfur species in aerosol and rainwater at a coastal site in New Zealand, *J. Geophys. Res.*, 101, 21 041–21 049, 1996.

Yin, F., Grosjean, D., and Seinfeld, J. H.: Photooxidation of dimethylsulfide and dimethyldisulfide: mechanism development, *J. Atmos. Chem.*, 11, 309–364, 1990.

Gaseous and particulate sulfur species

H. Bardouki et al.

Table 1. Observed mean mixing ratios of DMS and the other gaseous and particulate S species during the campaign (SD=standard deviation, n=number of data). The mean values for MSA and H₂SO₄ have been calculated using hourly data

Compound	n	Mean	SD	Median
(pmol·mol ⁻¹)				
DMS	490	21.7	21.5	15.2
DMSO	201	1.66	1.74	1.20
MS ⁻	224	11.5	5.8	10.4
SO ²	220	1030	600	910
nss-SO ₄ ²⁻	220	1440	760	1300
(molecules cm ⁻³)				
MSAg	3453	5.2×10 ⁵	2.5×10 ⁶	1.1×10 ⁵
H ₂ SO _{4g}	674	1.0×10 ⁷	1.7×10 ⁷	1.8×10 ⁶

[Title Page](#)
[Abstract](#)
[Introduction](#)
[Conclusions](#)
[References](#)
[Tables](#)
[Figures](#)
[◀](#)
[▶](#)
[◀](#)
[▶](#)
[Back](#)
[Close](#)
[Full Screen / Esc](#)
[Print Version](#)
[Interactive Discussion](#)

© EGU 2003

Gaseous and particulate sulfur species

H. Bardouki et al.

Table 2. Daily variation of k_{cs} (s^{-1}) and the corresponding r^2 , obtained by plotting $k [SO_2] [OH]$ as a function of $[H_2SO_4]$

Date	k_{cs} (s^{-1})	r^2
7/8/2001	0.0089	0.94
8/8/2001	0.0084	0.94
9/8/2001	0.0086	0.95
10/8/2001	0.0133	0.98
11/8/2001	0.0122	0.98
12/8/2001	0.0071	0.70
13/8/2001	0.0087	0.86
14/8/2001	0.0114	0.98
15/8/2001	0.0148	0.94
16/8/2001	0.0167	0.74
17/8/2001	0.0129	0.71
18/8/2001	0.0149	0.98
19/8/2001	0.0144	1.00
20/8/2001	0.0134	0.84
21/8/2001	0.0072	0.98

Title Page

Abstract

Introduction

Conclusions

References

Tables

Figures

◀

▶

◀

▶

Back

Close

Full Screen / Esc

Print Version

Interactive Discussion

© EGU 2003

Gaseous and particulate sulfur species

H. Bardouki et al.

Table 3. MSA yield (Y) derived during the experiment by using the equation $k [\text{DMS}] [\text{OH}] [\text{Y}] = k_{\text{CS}} [\text{MSA}]$ and the corresponding r^2

Date	MSA yield* per mil (‰)	r^2	MSA yield** per mil (‰)	r^2
10/8/2001	1.2	0.98	–	–
11/8/2001	1.5	0.67	–	–
14/8/2001	3.4	0.88	4.2	0.56
15/8/2001	2.8	0.93	3.0	0.75
16/8/2001	–	–	1.0	0.65
17/8/2001	–	–	1.3	0.78
18/8/2001	–	–	1.0	0.88

* = k_{CS} derived using the Fuchs-Sutugin equation (Fuchs and Sutugin, 1970)

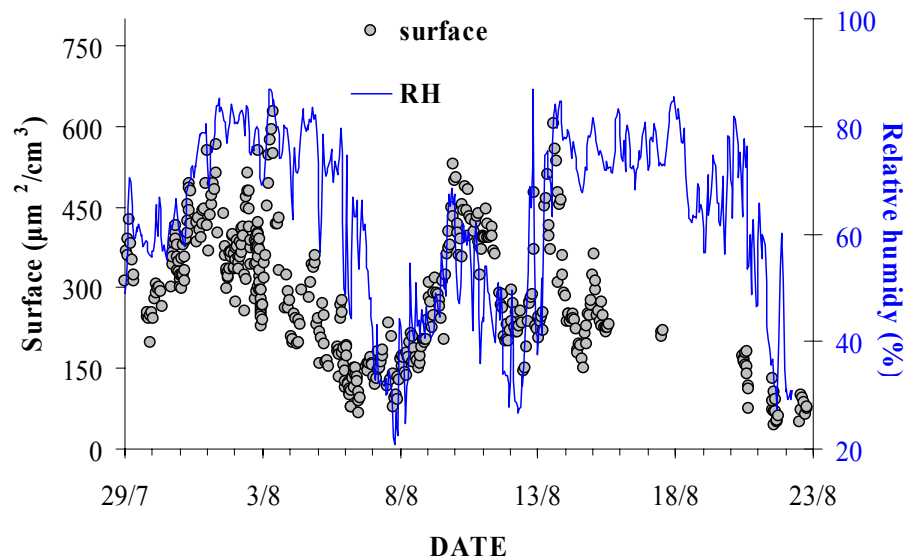
** = k_{CS} derived from H_2SO_4 data but corrected using an accommodation coefficient “ α ” for MSA equal to 0.075 as derived from the equation of De Bruyn et al. (1994).

[Title Page](#)
[Abstract](#)
[Introduction](#)
[Conclusions](#)
[References](#)
[Tables](#)
[Figures](#)
[◀](#)
[▶](#)
[◀](#)
[▶](#)
[Back](#)
[Close](#)
[Full Screen / Esc](#)
[Print Version](#)
[Interactive Discussion](#)

© EGU 2003

**Gaseous and
particulate sulfur
species**

H. Bardouki et al.

**Fig. 1.** Variation of aerosol surface data and RH during the campaign.[Title Page](#)[Abstract](#)[Introduction](#)[Conclusions](#)[References](#)[Tables](#)[Figures](#)[◀](#)[▶](#)[◀](#)[▶](#)[Back](#)[Close](#)[Full Screen / Esc](#)[Print Version](#)[Interactive Discussion](#)

© EGU 2003

Gaseous and
particulate sulfur
species

H. Bardouki et al.

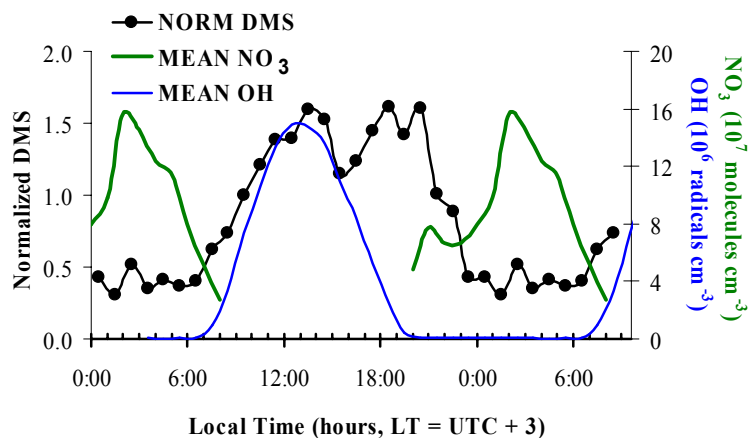
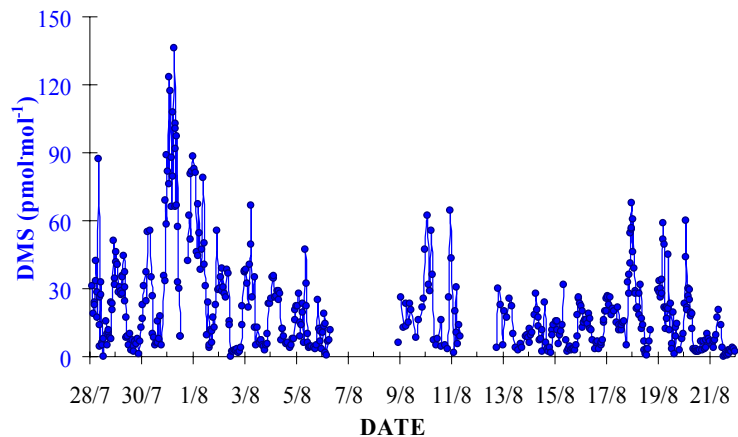


Fig. 2. Atmospheric concentrations of (a) DMS during the campaign and b) diurnal variation of normalized DMS ($\text{Normalized DMS} = \text{DMS}_{(\text{time,y,dayx})} / \text{mean DMS}_{(\text{dayx})}$) in relation to the mean OH and NO_3 levels measured during the campaign. Time refers to local time ($\text{LT} = \text{UT} + 3$).

[Title Page](#)[Abstract](#)[Introduction](#)[Conclusions](#)[References](#)[Tables](#)[Figures](#)[◀](#)[▶](#)[◀](#)[▶](#)[Back](#)[Close](#)[Full Screen / Esc](#)[Print Version](#)[Interactive Discussion](#)

© EGU 2003

Gaseous and
particulate sulfur
species

H. Bardouki et al.

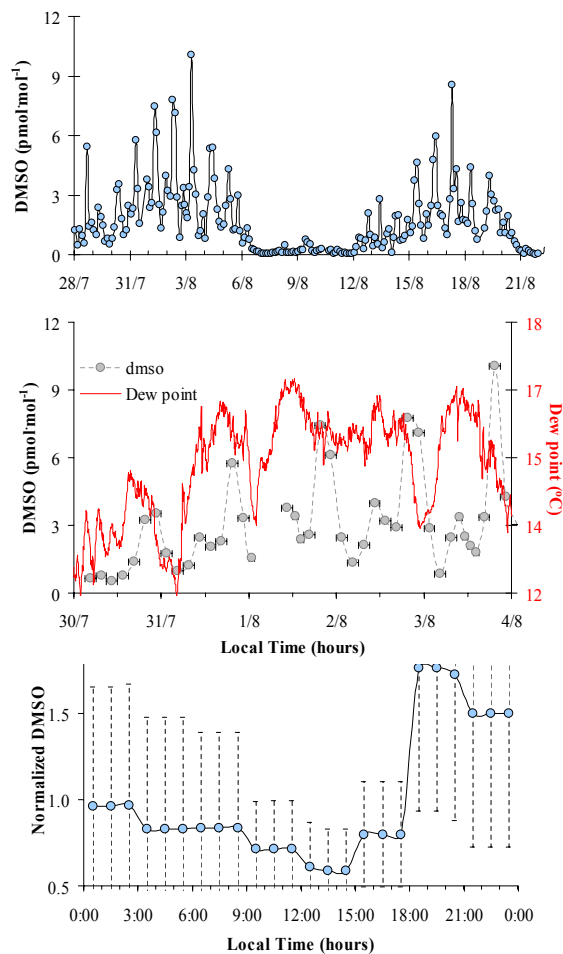


Fig. 3. Atmospheric concentrations of (a) DMSO, (b) variation of DMSO and RH and (c) diurnal variation of DMSO during the campaign.

[Title Page](#)[Abstract](#)[Introduction](#)[Conclusions](#)[References](#)[Tables](#)[Figures](#)[◀](#)[▶](#)[◀](#)[▶](#)[Back](#)[Close](#)[Full Screen / Esc](#)[Print Version](#)[Interactive Discussion](#)

**Gaseous and
particulate sulfur
species**

H. Bardouki et al.

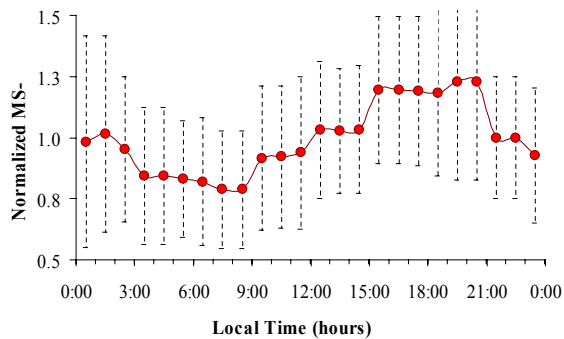
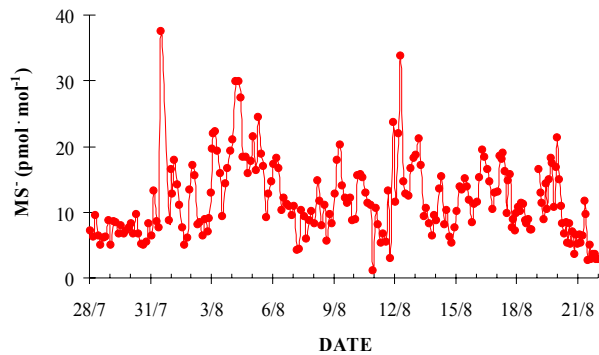


Fig. 4. Atmospheric concentrations of **(a)** MS^- and **(b)** diurnal profile of MS^- during the campaign.

[Title Page](#)[Abstract](#)[Introduction](#)[Conclusions](#)[References](#)[Tables](#)[Figures](#)[◀](#)[▶](#)[◀](#)[▶](#)[Back](#)[Close](#)[Full Screen / Esc](#)[Print Version](#)[Interactive Discussion](#)

© EGU 2003

**Gaseous and
particulate sulfur
species**

H. Bardouki et al.

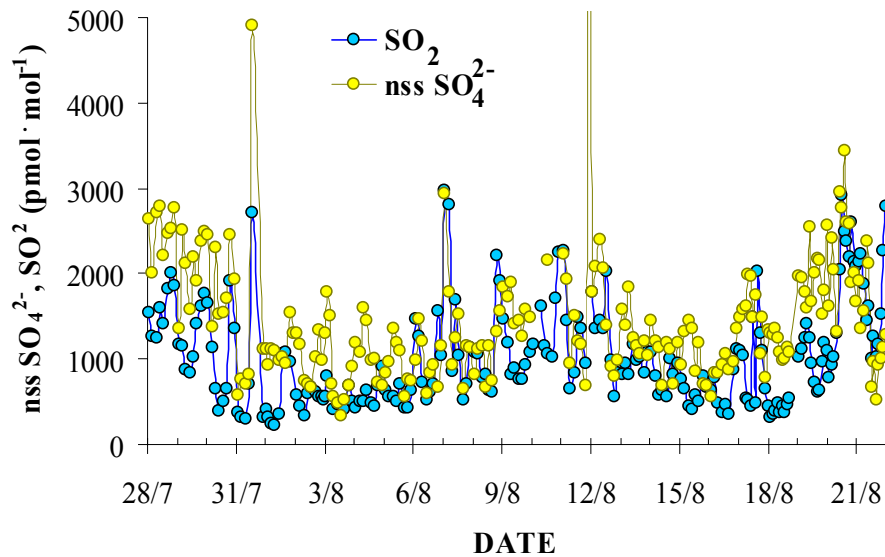


Fig. 5. Variability of SO_2 and nss-SO_4^{2-} during the campaign.

[Title Page](#)[Abstract](#)[Introduction](#)[Conclusions](#)[References](#)[Tables](#)[Figures](#)[◀](#)[▶](#)[◀](#)[▶](#)[Back](#)[Close](#)[Full Screen / Esc](#)[Print Version](#)[Interactive Discussion](#)

© EGU 2003

**Gaseous and
particulate sulfur
species**

H. Bardouki et al.

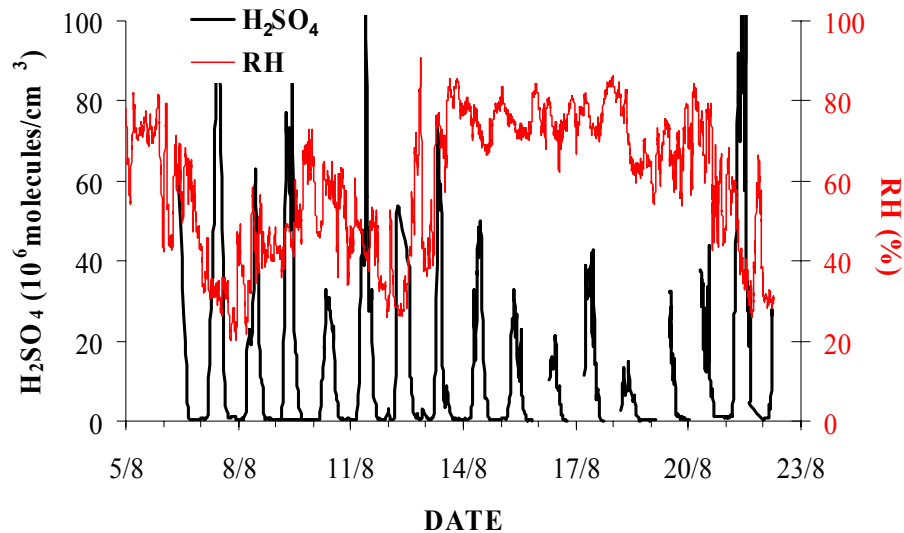


Fig. 6. Variation of atmospheric molecular concentrations of H₂SO₄ and RH during the campaign.

[Title Page](#)[Abstract](#)[Introduction](#)[Conclusions](#)[References](#)[Tables](#)[Figures](#)[◀](#)[▶](#)[◀](#)[▶](#)[Back](#)[Close](#)[Full Screen / Esc](#)[Print Version](#)[Interactive Discussion](#)

© EGU 2003

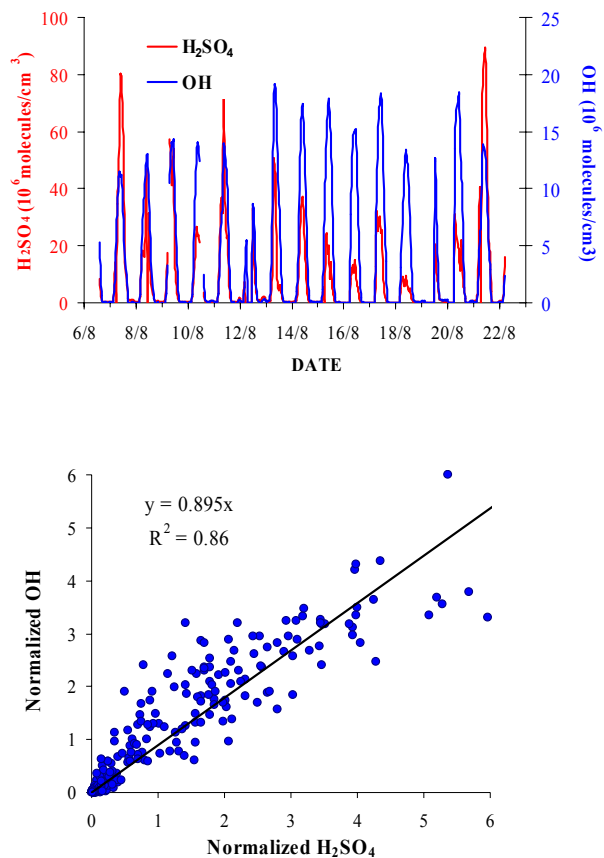


Fig. 7. Variation of (a) hourly means atmospheric molecular concentrations of H_2SO_4 and OH radicals and (b) regression between normalized H_2SO_4 and OH levels during the campaign.

[Title Page](#)[Abstract](#)[Introduction](#)[Conclusions](#)[References](#)[Tables](#)[Figures](#)[◀](#)[▶](#)[◀](#)[▶](#)[Back](#)[Close](#)[Full Screen / Esc](#)[Print Version](#)[Interactive Discussion](#)

© EGU 2003

Gaseous and
particulate sulfur
species

H. Bardouki et al.

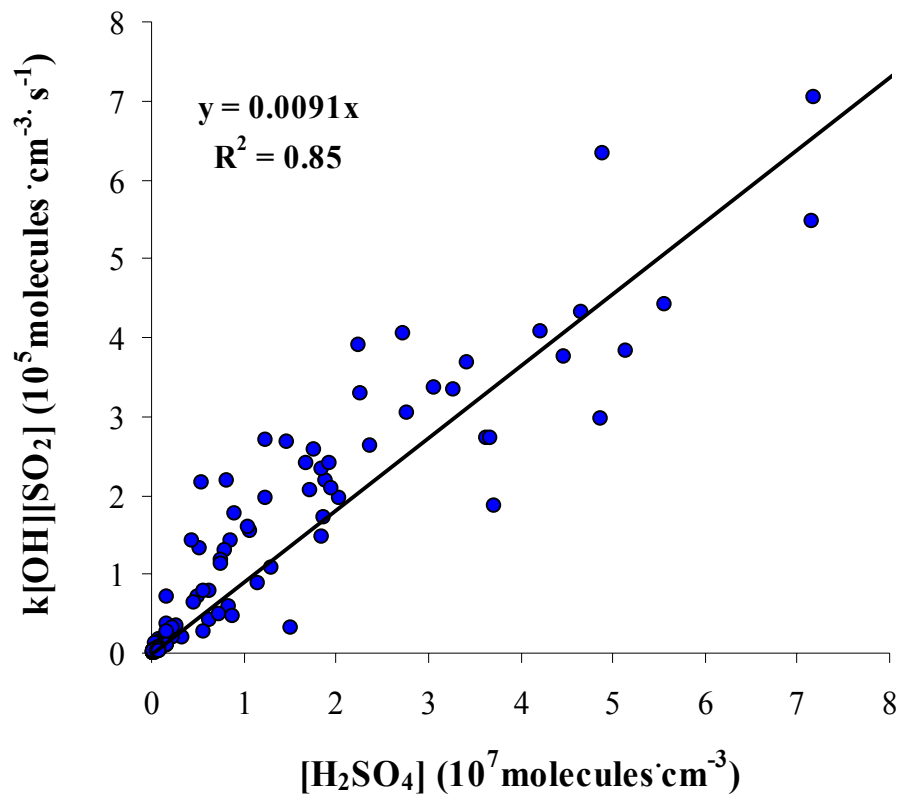


Fig. 8. Regression between $k[OH][SO_2]$ and $[H_2SO_4]$ during the campaign. The slope corresponds to k_{cs} of H_2SO_4 . OH and H_2SO_4 values averaged corresponding to SO_2 sampling integration times (typically 2–3 h).

[Title Page](#)[Abstract](#)[Introduction](#)[Conclusions](#)[References](#)[Tables](#)[Figures](#)[◀](#)[▶](#)[◀](#)[▶](#)[Back](#)[Close](#)[Full Screen / Esc](#)[Print Version](#)[Interactive Discussion](#)

© EGU 2003

Gaseous and
particulate sulfur
species

H. Bardouki et al.

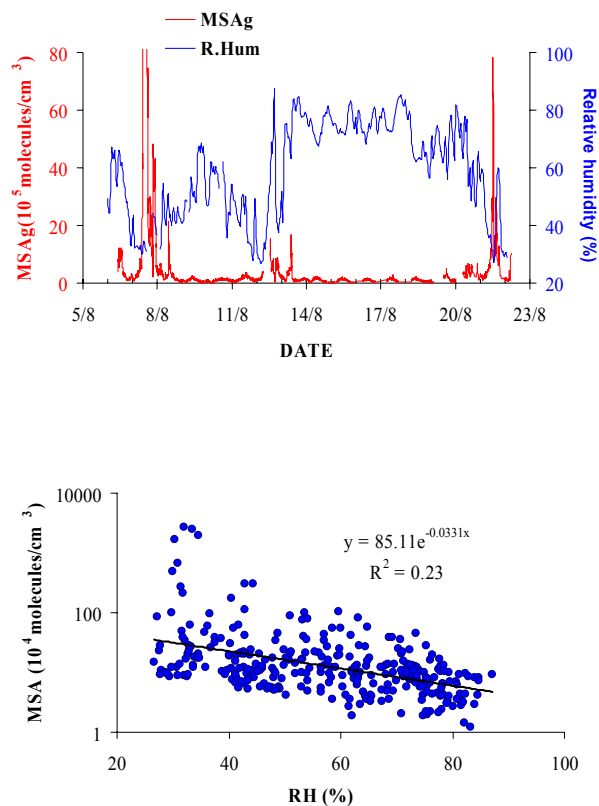


Fig. 9. Variation of (a) atmospheric molecular concentrations of MSAg and RH and (b) regression between MSAg and RH during the campaign.

[Title Page](#)[Abstract](#)[Introduction](#)[Conclusions](#)[References](#)[Tables](#)[Figures](#)[◀](#)[▶](#)[◀](#)[▶](#)[Back](#)[Close](#)[Full Screen / Esc](#)[Print Version](#)[Interactive Discussion](#)

© EGU 2003

Gaseous and
particulate sulfur
species

H. Bardouki et al.

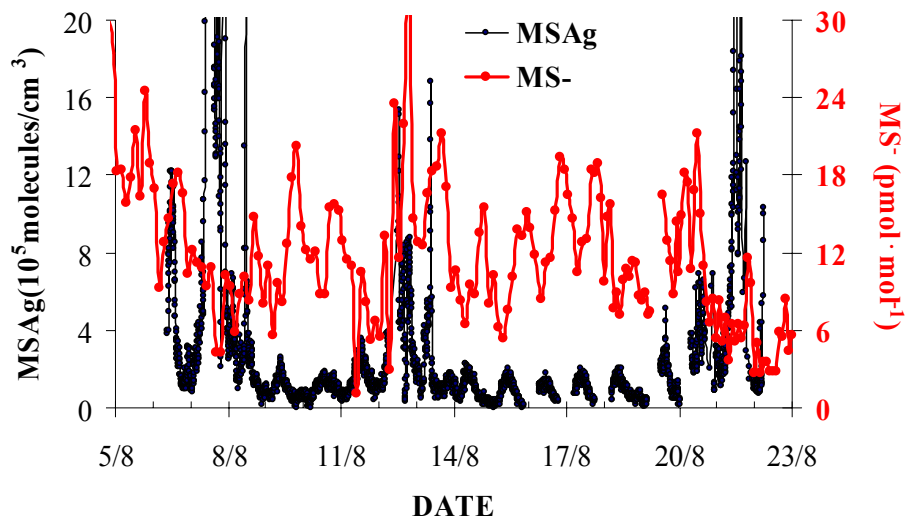


Fig. 10. Variation of atmospheric molecular concentrations of MSAg and aerosol MS^- during the campaign.

[Title Page](#)[Abstract](#)[Introduction](#)[Conclusions](#)[References](#)[Tables](#)[Figures](#)[◀](#)[▶](#)[◀](#)[▶](#)[Back](#)[Close](#)[Full Screen / Esc](#)[Print Version](#)[Interactive Discussion](#)

© EGU 2003

Gaseous and
particulate sulfur
species

H. Bardouki et al.

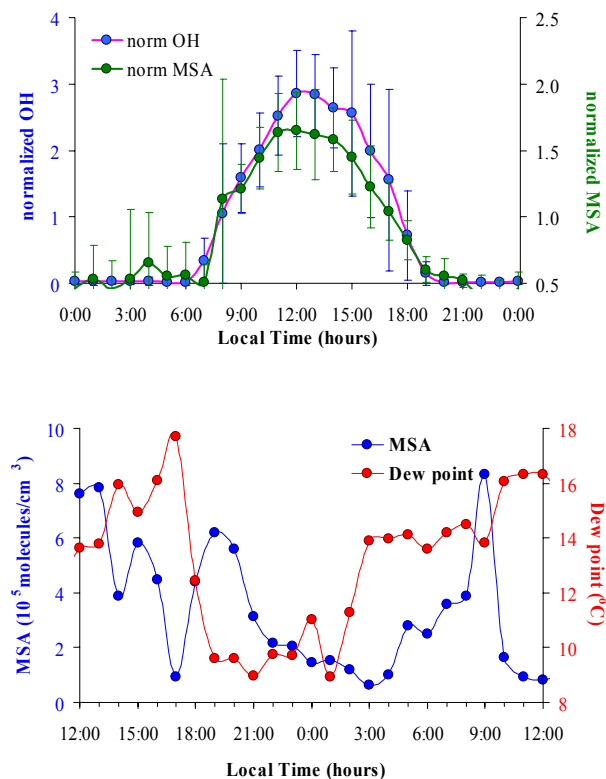


Fig. 11. Normalized profiles of MSA during two cases: **(a)** during periods with elevated (>40%) RH and **(b)** during a day with low RH (12–13 August). The variation of dew point is also plotted during the second case.

[Title Page](#)[Abstract](#)[Introduction](#)[Conclusions](#)[References](#)[Tables](#)[Figures](#)[◀](#)[▶](#)[◀](#)[▶](#)[Back](#)[Close](#)[Full Screen / Esc](#)[Print Version](#)[Interactive Discussion](#)

© EGU 2003